ORIGINAL RESEARCH

# Iron Particle–Enhanced Visualization of Inflammatory Central Nervous System Lesions by High Resolution: Preliminary Data in an Animal Model

R.A. Linker
A. Kroner
T. Horn
R. Gold
M. Mäurer
M. Bendszus

**BACKGROUND AND PURPOSE:** The detection of cell infiltration is critical for the diagnosis and monitoring of inflammatory disorders, especially in the central nervous system (CNS). Superparamagnetic iron oxide (SPIO) particles have recently been introduced as a contrast agent to detect macrophage migration in vivo by MR imaging. We tested the hypothesis that focal hyperechogenicity due to SPIO-laden macrophages can also be visualized on high-resolution sonography.

**METHODS:** Experimental autoimmune encephalomyelitis (EAE) was induced by myelin-oligodendrocyte glycoprotein (MOG) in congenic Lewis rats, an animal model mimicking many aspects of human multiple sclerosis. At the height of disease, rats underwent MR imaging with a 1.5T unit. Animals were injected with SPIO particles 24 hours before imaging. Control rats either received no contrast agent or were injected with SPIO particles without prior induction of EAE. Immediately after MR imaging, the rats were sacrificed, and the brains were removed and placed in saline. Sonography was performed directly after brain removal. Brains were embedded in paraffin, and sections were stained for iron with Perls stain and for macrophages with ED1 immunohistochemistry.

**RESULTS:** SPIO-enhanced sonography of rat brains during a relapse of EAE specifically showed marked focal echogenicity in EAE-typical areas of the brain, including the periventricular region, the cerebellum, and the brain stem. The sonographic results corresponded to in vivo MR imaging findings of the respective animals as well to the clinical symptoms of EAE and to histology showing iron-laden macrophages in demyelinated lesions.

**CONCLUSION:** SPIO particles allow the detection and demarcation of inflammatory CNS lesions on sonograms by specific macrophage imaging.



Two- and 3D imaging by sonography is a widely used real-time method for noninvasive analysis of various tissue alterations. In the central nervous system (CNS), B-mode sonography can routinely be applied to detect tumor growth or to evaluate ventricular diameters (eg, as a surrogate parameter to determine brain atrophy in multiple sclerosis).[1,2] Iron can be detected by sonography, as shown previously in animal models and in patients with Parkinson disease.[3,4] A direct visualization of inflammatory lesions in the brain by sonography has not been feasible so far. Recently, the development of more specific molecular and cellular imaging approaches has been an important issue in medical sonography research.[5]

Cell-type specific imaging of macrophages is already possible by MR imaging after the application of superparamagnetic iron oxide (SPIO) particles,[6] which specifically accumulate in phagocytic cells.[7] Preliminary studies have shown that SPIO-enhanced MR imaging allows the detection of macrophages in inflammatory CNS lesions.[8] Moreover, macrophage visualization on MR imaging has been shown in animal models of tumor, nerve trauma, brain ischemia, and autoimmune neuritis.[7,9-11]

Received July 5, 2005; accepted after revision October 17.

From the Clinical Research Group for Multiple Sclerosis (R.A.L., A.K., R.G., M.M.), Departments of Neurology and Neuroradiology (T.H., M.B.), Julius Maximilians-Universität Würzburg, Germany; and the Institute for Multiple Sclerosis Research (R.A.L., R.G.), University of Göttingen and gemeinnützige Hertie-Stiftung, Waldweg, Germany.

The authors received Resovist from Bernd Misselwitz, MD, Schering AG, Berlin. M.B. holds a "Stiftungsprofessur" supported by a grant from Schering Deutschland GmbH, Berlin.

Please address correspondence to: Mathias Mäurer, MD, Neurologische Universitätsklinik Würzburg, Josef-Schneider-Str. 11, 97080 Würzburg.

As a paradigm for CNS inflammation, we chose experimental autoimmune encephalomyelitis (EAE), a prototype T-cell–mediated autoimmune disease of the CNS, which is histopathologically characterized by demyelination, axonal damage, and inflammation, the most prevalent cell type being macrophages.[12] We focused on a chronic relapsing demyelinating disease model induced by immunization with myelin oligodendrocyte glycoprotein (MOG) in congenic Lewis rats.[13] Here, we investigated the potential of high-resolution sonography by using SPIO particles as a contrast agent to delineate inflammatory CNS lesions and to compare sonography with MR imaging.

## Methods

### *Induction of EAE and SPIO-Particle Injection Protocol*

1AV1 congenic Lewis rats were obtained from the University of Hanover and bred and housed at the in-house animal care facilities at the Department of Neurology, Würzburg. All experiments were approved by the local Bavarian state authorities. Six- to 8-week-old 1AV1 rats with body weights ranging from 140–180 g were immunized with 50 $\mu$g of recombinant human myelin-oligodendrocyte glycoprotein (rhMOG) protein (prepared after being emulsified in 75 $\mu$g of Freund's complete adjuvant).[14] The resulting EAE course is chronic with superimposed relapses and mimics many clinical and histopathologic features of the human disease multiple sclerosis with a predominant macrophage infiltration.[15] Animals were weighed and their disease state was scored according to clinical signs, on a daily basis. Animals were examined at the height of disease. According to disease severity, rats were stratified into 3 groups. In the first group, 1

mmol of iron per kg of body weight of SPIO particles (Resovist, Schering, Berlin, Germany) was administered intravenously 24 hours before every MR imaging and sonographic examination ($n = 4$, animals pooled from 2 independent experiments). In the second and third groups, 6 control rats received either phosphate buffered saline (PBS) after induction of EAE as described previously ($n = 3$) or 1 mmol of iron per kg of body weight of SPIO particles without prior induction of EAE ($n = 3$). In dose titration experiments, 0.2 mmol of iron per kg of body weight was used.

### *MR Imaging Protocol*

All measurements were performed on a clinical 1.5T MR imaging unit (Magnetom Vision, Siemens, Erlangen, Germany). Before the MR imaging measurements were obtained, rats were anesthetized by intraperitoneal injection of 100 mg per kg of body weight of ketamine (Ketanest) and 10 mg per kg of body weight of xylazin (Rompun). For all MR imaging examinations, animals were in a supine position with their heads fixed in a round surface coil (40 mm in diameter). The MR imaging protocol included T1-weighted (TR/TE, 460/14 ms) and T2-weighted (TR/TE, 2500/80 ms) sequences in the coronal plane with a section thickness of 3 mm. Moreover, a 3D-constructed interference in steady state (CISS; TR/TE, 16.4/8.2 ms) sequence was applied in the coronal plane with a section thickness of 1 mm.[16]

### *Sonographic Examination*

Following MR imaging, rats were killed by $CO_2$ narcosis, and the brains were rapidly and carefully removed and placed into a water tank. Sonography was performed ex vivo by using a color-coded phased-array sonographic system equipped with a VX 13.5 13-MHz transducer (Sonoline Elegra, Siemens) with an emission frequency of 12 MHz. The axial resolution in the focus zone was approximately 0.7 mm. The sonographic system indices chosen were penetration depth, 1.5 cm; dynamic range, 60 dB; low persistence; and focus length, 1 cm. Image brightness and gain (26 dB) were not changed for sonification of the different groups. The sonographic transducer was fixed above the water tank, and the brain was imaged in coronal planes and a rostrocaudal direction by continuously moving the tank underneath the transducer with a mechanical table.

### *Histology*

After sonography, brains were immersion-fixed for 2 hours in 4% paraformaldehyde, washed in tris-hydroxymethyl aminomethane–buffered saline (TBS), and embedded in paraffin. Subsequently, 5-$\mu$m-thick paraffin sections were cut at multiple levels through the lesions as detected on MR imaging and sonography, deparaffinized with xylene, rehydrated, and washed in water and TBS. For iron detection, tissue sections were rinsed in deionized water and immersed in Perls solution containing 2% potassium ferrocyanide and 2% hydrochloride at a 1:1 concentration for 30 minutes. Sections were then rinsed in deionized water and either dehydrated and cover slipped or further processed for ED1 immunocytochemistry. Additional sections were only stained by immunocytochemistry by using the antibody ED1 at a dilution of 1:1000, as a marker for monocytes/macrophages and phagocytic microglia (MCA 341R; Serotec, Oxford, UK). Binding of ED1 antibodies to cells was visualized by the avidin-biotin-peroxidase method with diaminobenzidine as a chromogen, according to routine procedures.[17] For unequivocal identification of iron-labeled cells, Perls stain and ED1 immunocytochemistry were performed on the same sections. Sections were examined with a Zeiss-Axiophot microscope (Zeiss, Stuttgart, Germany).

## Results

Induction of recombinant human MOG-EAE in congenic 1AV1 Lewis rats resulted in a severe disease course with tetraparesis or prominent ataxia 12 days after immunization. At that time point, sonography of the brains 24 hours after application of SPIO particles revealed circumscribed and sharply delineated areas of marked echogenicity in a frontal and periventricular distribution or location in the brain stem or cerebellum, respectively (Fig 1, upper row). The pattern of echogenicity correlated well with the clinical symptoms of individual animals: Tetraparetic rats had brain stem lesions; a severely ataxic animal showed a cerebellar lesion.

In contrast, sonography of brains from EAE-diseased rats after injection of PBS or healthy control rats 24 hours after injection of identical SPIO particle doses revealed no similar focal hyperechogenicity (compare Fig 1, upper row, with Fig 1, middle and lower rows). Application of a lower dose of SPIO particles (0.2 mmol per kg of body weight) gave a similar result, with circumscribed echogenic lesions depicted on the sonography of the brain and spinal cord (data not shown).

To compare the sonographic findings with an established technique for noninvasive lesion detection in inflammatory CNS diseases, we performed in vivo MR imaging before sonography. MR imaging revealed focal areas of signal-intensity loss on T2-weighted and CISS images (Fig 2*D–F*), which are indicative of local accumulation of SPIO particles in corresponding areas of hyperechogenicity on sonography. Equivalent to the distribution of lesions in sonography, all SPIO-enhanced lesions could also be detected on MR imaging, in periventricular areas as well as in the cerebellar or brain stem region. The extent of the signal intensity loss could best be demonstrated on high-resolution CISS images. Imaging of healthy control rats after application of SPIO particles did not demonstrate areas of focal signal-intensity loss. All lesions seen on MR imaging were also found on sonography by an observer masked to the MR imaging results; this result attests to the specificity of our sonographic findings.

We aimed to confirm our imaging results by histologic evaluation of regions with focal sonographic/MR imaging abnormalities. Immunostaining with ED1 as a marker for phagocytic monocytes/macrophages revealed extensive perivascular and intraparenchymal macrophage infiltration in the regions of interest (Fig 3*A*). In confirmation of our sonographic and MR imaging findings, we could demonstrate focal iron deposition in sequential histologic sections stained with Perls solution (Fig 3*B*). The nature of iron-laden cells in inflammatory brain lesions could be identified by immersion in Perls stain for iron detection and subsequently processing for ED1 immunostaining, revealing clear colocalisation and thereby identifying macrophage-like cells as definitively iron-laden cell types in the CNS (Fig 3*C*).

Perls staining of liver sections with massively iron-laden Kupffer cells served as a histologically positive control for correct intravenous SPIO-particle injection (Fig 3*B,* inset).

## Discussion

Here we applied sonography for macrophage-specific imaging of inflammatory CNS lesions by using SPIO particles. In vivo labeling of macrophages by iron particles has already been demonstrated by MR imaging.[7-9] Previous experimental and

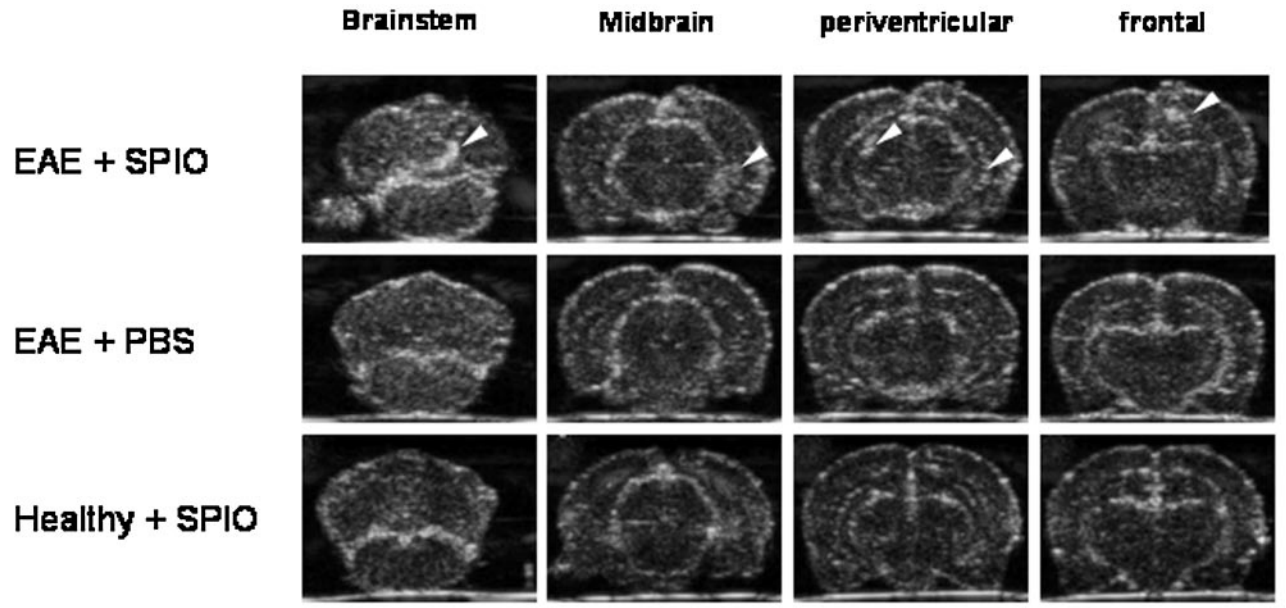


**Fig 1.** SPIO-based macrophage imaging in EAE lesions of the rat brain by sonography. rhMOG-EAE was induced in congenic 1AV1 Lewis rats. During relapse, whole brains were removed and imaged ex vivo in a water tank by using a 13-MHz phased-array sonographic transducer 24 hours after SPIO injection. On coronal planes, sharply delineated circumscribed areas of focal echogenicity could be identified in different rats, predominantly involving the frontal, periventricular, cerebellar, and brain stem region (upper row, lesions marked by *white arrows*; representative images from different rats are shown), a pattern that is typical for MOG-EAE. Imaging of rat brains with injection of PBS after induction of rhMOG-EAE (middle row, anatomically equivalent areas from different rats are shown) or SPIO injection without prior induction of EAE (lower row) did not reveal similar areas with focal hyperechogenicity and served as negative controls.

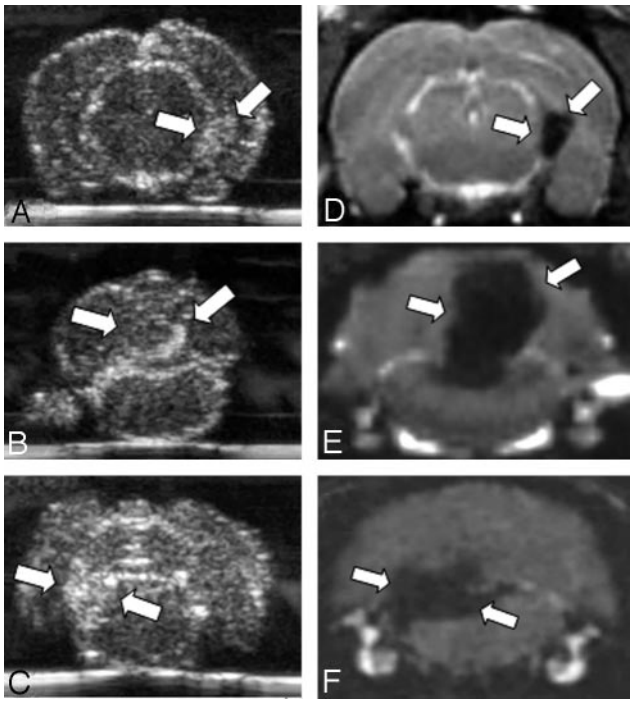


**Fig 2.** Comparison of SPIO-enhanced sonographic imaging of EAE lesions with MR imaging. We performed in vivo MR imaging to correlate the sonographic results with a well-established technique to monitor SPIO-particle accumulation. On coronal CISS images (*D–F*) corresponding to the brain regions depicted by sonography (*A–C*), we identified areas of focal hypointensity in the periventricular area (*A, -D*) and in the cerebellar (*B, -E*) or brain stem region (*C, -F*) of rat brains (lesions marked by *white arrows*). Hypointense areas are indicative of local SPIO-particle accumulation. Note the marked similarity of lesion distribution between sonograms and MR images (compare *A–C* with *D–F*).

clinical studies have shown an increase of tissue echogenicity on sonograms because of local iron deposition. Stereotactically injected ferric chloride into rat substantia nigra causes hyperechogenicity.[3] In a postmortem brain analysis of 20 patients without extrapyramidal disorders, hyperechogenicity of the substantia nigra on sonography was related to a higher tissue iron level.[4] The present study shows that accumulation of iron-laden macrophages can lead to increased echogenicity on sonograms. Echogenicity may result from packed iron deposits in macrophages, which, altogether, create a front of small scatterers, whereas single SPIO particles in the nanometer range may be well below the detection threshold for sonography.

Although increased cell attenuation can sometimes lead to increased echogenicity in sonography,[18] this effect is not sufficient to properly identify inflammatory lesions in the present case because imaging of EAE brains without prior injection of SPIO fails to reproducibly delineate similar lesions, such as those seen after SPIO injection. The specificity of our findings was confirmed by corresponding results on MR imaging and histology. All lesions detected by MR imaging could also be delineated on sonography by a blinded observer. These results strongly argue for a specific imaging of iron-laden macrophages with our sonographic approach. Although lesion localization was similar, lesion size and shape could, in fact, differ between sonography and MR imaging (compare Fig 2*B* and *E*). The actual extent of lesions as proved by histology was more closely reflected on sonograms. A possible reason for this mismatch might be oversizing at MR imaging because of signal-intensity annihilation.

Moreover, we used relatively high SPIO dosages in the first experiments to assure a sufficient signal intensity. Preliminary dose titration studies indicate that similar results are also feasible with lower SPIO dosages (0.2 mmol per kg of body weight). In the future, we will perform additional in vivo studies with iron particles at different dosages to assess the feasi-

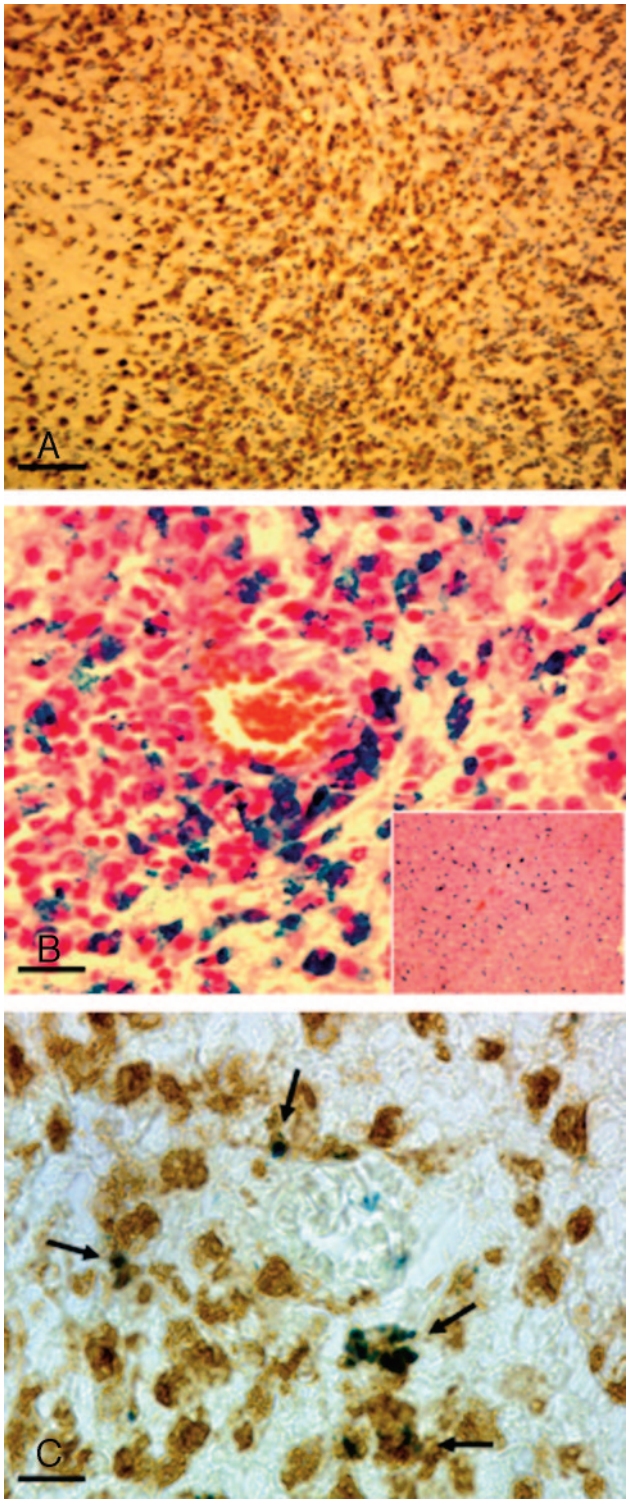


**Fig 3.** Histologic evaluation. Paraffin sections were cut through the lesions as detected on MR imaging and sonography. *A* and *B*, The histology corresponds to the cerebellar lesion depicted in Figs 1*A* and 2*A*. *A*, Staining of macrophages and activated microglia by immunohistochemistry for ED1 (bar = 50 $\mu$m). Note the massive infiltrate of brown-stained ED1–positive cells. On a consecutive section (*B*, bar = 15 $\mu$m), Perls blue staining was performed to detect focal iron accumulation. Note the extensive perivascular iron deposition. Perls staining of liver sections with massively iron-laden Kupffer cells served as a histologically positive control for correct intravenous SPIO-particle injection (*B*, inset). Combination of Perls staining with ED1 immunohistochemistry reveals a clear colocalisation (*C*, bar = 10 $\mu$m), thereby identifying macrophage-like cells as one of the definitively iron-laden cell types in the CNS.

bility of in vivo detection of iron particles by sonography in the CNS.

One drawback of the present study is the ex vivo design. However, it was recently possible to perform sonography through the intact rodent skull with antibody-conjugated gas-filled microbubbles as a contrast agent[19]; this procedure shows that in vivo imaging in rodents is feasible with advanced sonographic technology.

SPIO particles are already in clinical use for MR imaging of liver disease.[20] In this condition, the feasibility of sonography after SPIO injection has already been described in humans.[21] Yet, the use of intravenous injection of SPIO for diagnosing inflammation on sonography must become more sensitive and specific before it can be applied routinely. In a first step, iron-enhanced sonography may serve more as a complementary rather than an entirely competitive approach to SPIO-enhanced MR imaging.

SPIO-based sonography may evolve to be of particular interest to diagnose CNS inflammation in neonatal imaging. Postnatal transcranial sonography is already a widely used technique because of its portability, low cost, minimal morbidity, and diagnostic image quality.[22] Sonographic changes in brain parenchyma or extracerebral fluid and ventricles of the neonate have been described, in particular with inflammatory conditions like cerebritis, abscess, empyema, or ventriculitis; but also edema, hemorrhage, infarction, or hydrocephalus can be identified. With the imaging of iron accumulation as a marker for macrophage infiltration, SPIO-enhanced sonography may provide valuable information in making the diagnosis, identifying complications, and directing decisions in management of CNS inflammation. Yet, in the neonate, the issue of iron toxicity will have to be critically considered.

## Conclusion

Intravenous injection of SPIO particles allows the detection and demarcation of inflammatory lesions on sonograms. This pilot ex vivo study reveals that iron-enhanced sonography is feasible for the detection of macrophage infiltration during autoimmunity of the CNS.

### *Acknowledgments*

We thank Verena Wörtmann, Katharina Teutlein, and Carolin Kiesel for their excellent and skillful technical assistance and Andreas Weishaupt, Department of Neurology, University of Würzburg, for preparation of the MOG protein.

## References

1. Berg D, Maurer M, Warmuth-Metz M, et al. **The correlation between ventricular diameter measured by transcranial sonography and clinical disability and cognitive dysfunction in patients with multiple sclerosis.** *Arch Neurol* 2000;57:1289–92
2. Kallmann BA, Sauer J, Schliesser M, et al. **Determination of ventricular diameters in multiple sclerosis patients with transcranial sonography (TCS): a two year follow-up study.** *J Neurol* 2004;251:30–34
3. Berg D, Grote C, Rausch WD, et al. **Iron accumulation in the substantia nigra in rats visualized by ultrasound.** *Ultrasound Med Biol* 1999;25:901–04
4. Berg D, Roggendorf W, Schroder U, et al. **Echogenicity of the substantia nigra: association with increased iron content and marker for susceptibility to nigrostriatal injury.** *Arch Neurol* 2002;59:999–1005
5. Dayton PA, Ferrara KW. **Targeted imaging using ultrasound.** *J Magn Reson Imaging* 2002;16:362–77
6. Weinmann HJ, Ebert W, Misselwitz B, et al. **Tissue-specific MR contrast agents.** *Eur J Radiol* 2003;46:33–44

7. Bendszus M, Stoll G. **Caught in the act: in vivo mapping of macrophage infiltration in nerve injury by magnetic resonance imaging.** *J Neurosci* 2003;23:10892–96
8. Dousset V, Ballarino L, Delalande C, et al. **Comparison of ultrasmall particles of iron oxide (USPIO)-enhanced T2-weighted, conventional T2-weighted, and gadolinium-enhanced T1-weighted MR images in rats with experimental autoimmune encephalomyelitis.** *AJNR Am J Neuroradiol* 1999;20:223–27
9. Kleinschnitz C, Bendszus M, Frank M, et al. **In vivo monitoring of macrophage infiltration in experimental ischemic brain lesions by magnetic resonance imaging.** *J Cereb Blood Flow Metab* 2003;23:1356–61
10. Stoll G, Wesemeier C, Gold R, et al. **In vivo monitoring of macrophage infiltration in experimental autoimmune neuritis by magnetic resonance imaging.** *J Neuroimmunol* 2004;149:142–46
11. Nolte I, Vince GH, Maurer M, et al. **Iron particles enhance visualization of experimental gliomas with high-resolution sonography.** *AJNR Am J Neuroradiol* 2005;26:1469–74
12. Bruck W, Porada P, Poser S, et al. **Monocyte/macrophage differentiation in early multiple sclerosis lesions.** *Ann Neurol* 1995;38:788–96
13. Gold R, Hartung HP, Toyka KV. **Animal models for autoimmune demyelinating disorders of the nervous system.** *Mol Med Today* 2000;6:88–91
14. Adelmann M, Wood J, Benzel I, et al. **The N-terminal domain of the myelin oligodendrocyte glycoprotein (MOG) induces acute demyelinating experimental autoimmune encephalomyelitis in the Lewis rat.** *J Neuroimmunol* 1995;63:17–27
15. Storch MK, Stefferl A, Brehm U, et al. **Autoimmunity to myelin oligodendrocyte glycoprotein in rats mimics the spectrum of multiple sclerosis pathology.** *Brain Pathol* 1998;8:681–94
16. Casselman JW, Kuhweide R, Deimling M, et al. **Constructive interference in steady state-3DFT MR imaging of the inner ear and cerebellopontine angle.** *AJNR Am J Neuroradiol* 1993;14:47–57
17. Linker RA, Maurer M, Gaupp S, et al. **CNTF is a major protective factor in demyelinating CNS disease: a neurotrophic cytokine as modulator in neuroinflammation** *Nat Med* 2002;8:620–24
18. Becker G, Krone A, Schmitt K, et al. **Preoperative and postoperative follow-up in high-grade gliomas: comparison of transcranial color-coded real-time sonography and computed tomography findings.** *Ultrasound Med Biol* 1995;21:1123–35
19. Reinhardt M, Hauff P, Linker RA, et al. **Ultrasound derived imaging and quantification of cell adhesion molecules in experimental autoimmune encephalomyelitis (EAE) by Sensitive Particle Acoustic Quantification (SPAQ).** *Neuroimage* 2005;27:267–78
20. Weinmann HJ, Ebert W, Misselwitz B, et al. **Tissue-specific MR contrast agents.** *Eur J Radiol* 2003;43:33–44
21. Tanzer H, Sigl G, Spiethoff T, et al. **Is iron oxide a tissue-specific contrast medium in diagnostic ultrasound? A case report.** *Ultraschall Med* 2004;25:448–49
22. Frank LM, White LE. **Neurosonographic features of central nervous system infections in infancy and childhood.** *J Child Neurol* 1989;4(suppl):S41–51